Selective Oxidation Control for Synchronous Vanadium Extraction and Chromium Retention from Vanadium- and Chromium-Bearing Hot Metal

Xin-yu Wang , Yuan-hong Qi * , Hai-quan Zhao , Lu-feng Wang , Qiao-chu Liu , Ding-liu Yan , Feng Wang

Posted Date: 22 October 2025

doi: 10.20944/preprints202510.1670.v1

Keywords: vanadium- and chromium-bearing hot metal; vanadium extraction; chromium retention; selective oxidation; resource utilization

Article

Selective Oxidation Control for Synchronous Vanadium Extraction and Chromium Retention from Vanadium- and Chromium-Bearing Hot Metal

Xin-yu Wang [1,2], Yuan-hong Qi [1,*], Hai-quan Zhao [2], Lu-feng Wang [2], Qiao-chu Liu [2], Ding-liu Yan [1] and Feng Wang [1]

[1] State Key Laboratory of Advanced Steel Processes and Products, CISRI, Beijing 100081, China

[2] College of Vanadium and Titanium, Panzhihua University, Panzhihua 617000, Sichuan, China

* Correspondence: qiyh0525_cn@sina.com

Abstract

To address the technical challenges in the resource utilization of hot metal containing high levels of vanadium (V: 2–5%) and chromium (Cr: 1–5%), this paper proposes a novel method based on pyrometallurgical selective oxidation for the simultaneous extraction of vanadium and retention of chromium. Through thermodynamic analysis and high-temperature smelting experiments, the competitive oxidation behaviors of carbon, vanadium, and chromium were revealed, and the synergistic control mechanism of temperature and oxygen partial pressure was clarified. The results indicate that within the temperature range of 1693–1753 K, vanadium preferentially oxidizes over carbon and chromium, while carbon effectively suppresses chromium oxidation. By optimizing the ω(FeO) (10.0–15.7%), achieving a vanadium oxidation efficiency (η_V) of 72.5–82.2% and maintaining the chromium retention efficiency (1–η_{Cr}) exceeding 57.1%. Compared to traditional methods—which rely on high-oxygen blowing (oxygen supply: 43–195 kg/tFe), multi-stage roasting, and hydrometallurgical refining—this approach eliminates roasting and hydrometallurgical steps, shortens the process chain, reduces oxygen consumption (> 80 kg/tFe), and lowers environmental risks (Cr oxidation reduced > 40%). The study establishes a theoretical framework for sustainable V/Cr separation, enhancing resource efficiency and minimizing pollution.

Keywords: vanadium- and chromium-bearing hot metal; vanadium extraction; chromium retention; selective oxidation; resource utilization

1. Introduction

Vanadium- and chromium-bearing hot metal is a product generated from the reduction and smelting of vanadium-extracted chromium-containing residues. Typically, its vanadium (V) content ranges from 2% to 5%, while its chromium (Cr) content ranges from 1% to 5% [1–4]. Due to the high content of V and Cr, there is still no effective way of resource utilization. The traditional separation process of V and Cr is oxidation enrichment-roasting pretreatment-wet separation. Although this process is highly industrialized, they are only applicable to low-vanadium and low-chromium hot metal (V: 0.15–0.35%, Cr: 0.2–0.6%) [4–6]. However, the availability of relevant research and experimental data remains severely limited for high-vanadium and high-chromium hot metal (V > 2%, Cr > 1%), and the applicability of traditional processes in this context has yet to be fully validated. Furthermore, traditional processes are characterized long flowsheets, with a progressive decrease in metal recovery rates at each stage. Consequently, the overall recovery rate of vanadium and chromium from hot metal to final products typically reaches only 60–80% [6,7]. During converter oxidation, the high oxygen potential leads to excessive chromium oxidation (Cr_2O_3 accounts for 5–10% of the slag phase) [8–10], significantly reducing the efficiency of chromium recovery. In roasting step, sodium roasting produces high-salt wastewater containing Na^+ (5–10 g/L) and NH_4^+ (2–3 g/L)

 doi:10.20944/preprints202510.1670.v1

[8,11,12], as well as toxic wastewater containing Cr(VI) (0.5–1.2 kg/t) [13,14]. Calcium roasting generates by-product of $CaSO_4$ slag containing 12–15% sulfur [15–17], which is difficult to utilize as a resource. Moreover, the roasting process consumes 10–15% of the slag weight in Na_2CO_3 or $CaCO_3$ [18], with energy consumption reaching 200–300 kWh/t of slag [11,19], significantly increasing costs. Additionally, the subsequent hydrometallurgical leaching-precipitation process is time-consuming (12–16 hours), with vanadium leaching rates of only 33–85%, leaving a portion of vanadium in the slag [16,20]. Therefore, traditional processes exhibit significant shortcomings in terms of economic efficiency and environmental sustainability.

To address these issues, this paper proposes a novel and efficient method for separating vanadium and chromium based on pyrometallurgical selective oxidation. This method targets high-vanadium and high-chromium hot metal (V: 2%–5%, Cr: 1%–5%), achieving vanadium-chromium separation during the converter oxidation stage by selectively oxidizing vanadium into the slag while retaining chromium in the hot metal (as shown in Figure 1). Thus, the subsequent roasting and wet processing processes are completely eliminated. The aim of this method is to provide a new technical path for the resource utilization of high vanadium and high chromium hot metal, and reduce the production cost, reduce the environmental pollution. To achieve these objectives, this study combines thermodynamic calculations with experimental verification. Through thermodynamic analysis, the oxidation behavior of carbon, vanadium, and chromium under different temperatures and oxygen potentials was elucidated, and the thermodynamic conditions for vanadium extraction and chromium retention were proposed. Based on these findings, high-temperature smelting experiments were designed to investigate the effects of temperature and oxygen potential on vanadium-chromium separation efficiency. The results demonstrate that this method maximizes vanadium oxidation while significantly reducing chromium oxidation. This study not only overcomes the technical bottleneck of selective oxidation in pyrometallurgical separation but also provides theoretical and practical guidance for the development of efficient and environmentally friendly metallurgical processes.

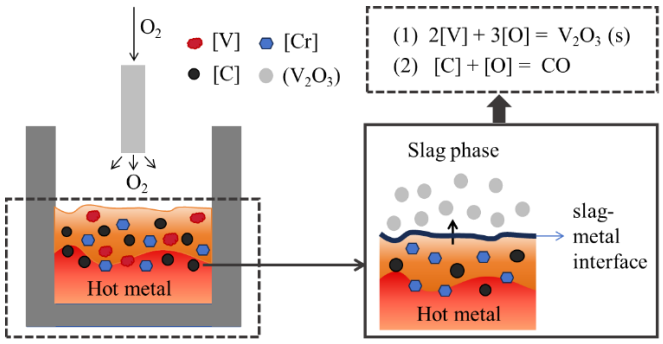

Figure 1. Schematic diagram.

2. Thermodynamic Analysis for Oxidative Vanadium Extraction and Chromium Retention in Hot Metal

2.1. Optimal Temperature Control Strategy

Under standard conditions, the oxidation reactions of vanadium, chromium, and carbon in vanadium- and chromium-bearing hot metal can be described by the following reaction Equations, and their corresponding Gibbs free energy changes ($\Delta G^{\ominus}$) [21] are also list:

$$2[O] + \frac{4}{3}[V] = \frac{4}{3}V_2O_3(s) \quad \Delta G_1^{\ominus} = -541.57 + 0.21T \ (kJ/mol) \tag{1}$$

$$2[O] + \frac{4}{3}[Cr] = \frac{4}{3}Cr_2O_3(s) \quad \Delta G_2^{\ominus} = -463.03 + 0.20T \ (kJ/mol) \tag{2}$$

$$2[O] + 2[C] = 2CO(g) \quad \Delta G_3^{\ominus} = 30.70 - 0.12T \ (kJ/mol) \tag{3}$$

 doi:10.20944/preprints202510.1670.v1

where $\Delta G_i^{\ominus}$ represents the standard Gibbs free energy change for reaction (i) (kJ/mol); i denotes the index of the chemical reaction, and T is the reaction temperature (K).

The temperature-dependent $\Delta G^{\ominus}$ of these reactions are plotted in Figure 2, the oxidation curve of carbon intersects with those of chromium and vanadium at points A (1517 K) and B (1704 K), respectively. By drawing vertical lines at these intersection points parallel to the Y-axis, the temperature domain is divided into three distinct regions: I (T < 1517 K), II (1517 K < T < 1704 K), and III (T > 1704 K).

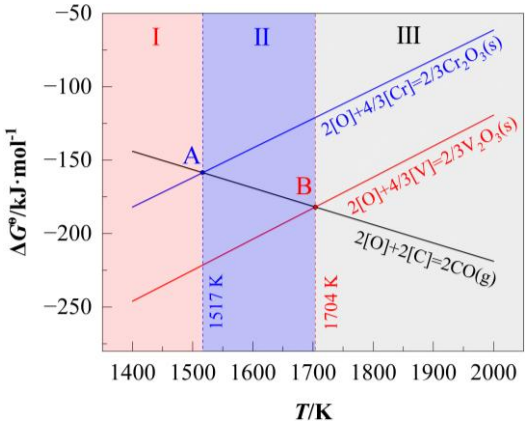

Figure 2. Relationship between $\Delta G^{\ominus}$ of oxidation reactions of [C], [V], and [Cr] and temperature under standard conditions.

- Region I (T < 1517 K):

Oxidation priority follows [V] > [Cr] > [C]. However, the minimal separation between vanadium and chromium oxidation curves ($\Delta G^{\ominus}$ = 57.9–64.1 kJ/mol) leads to simultaneous oxidation of chromium during vanadium extraction, resulting in suboptimal chromium retention.

- Region II (1517 K < T < 1704 K):

The oxidation propensity of carbon is intermediate between those of vanadium and Chromium, thereby allowing it to function as a redox mediator that promotes vanadium extraction while preserving chromium in the metallic phase. The carbon-mediated reactions involved in this process are given by Equations (4) and (5). For the system to achieve concurrent vanadium extraction and chromium retention, both reactions must proceed spontaneously in the forward direction. This dual role is essential for the selective extraction of vanadium while maintaining chromium in the metallic state.

$$\frac{2}{3}Cr_2O_3(s) + 2[C] = \frac{4}{3}[Cr] + 2CO(g) \quad \Delta G_4^{\ominus} = 493.73 - 0.32T \ (kJ/mol) \tag{4}$$

$$\frac{4}{3}[V] + 2CO(g) = \frac{2}{3}V_2O_3(s) + 2[C] \quad \Delta G_5^{\ominus} = -572.27 + 0.33T \ (kJ/mol) \tag{5}$$

- Region III (T > 1704 K):

Oxidation priority reverses to [C] > [V] > [Cr], where premature carbon oxidation depletes oxygen availability, severely limiting vanadium extraction efficiency.

While all three regimes satisfy the basic requirement of [V] > [Cr] oxidation priority, Regime II (1517–1704 K) uniquely balances vanadium extraction efficiency and chromium retention. The intermediate temperature range ensures: (1) Maximized vanadium oxidation: Dominance of $\Delta G_1^{\ominus}$ over $\Delta G_3^{\ominus}$ maintains thermodynamic favorability for vanadium extraction; (2) Effective chromium protection: Carbon acts as a sacrificial agent, oxidizing before chromium and reducing oxygen activity in the melt.

 doi:10.20944/preprints202510.1670.v1

2.2. Oxygen Partial Pressure Control

The typical chemical composition of vanadium-chromium-containing hot metal obtained through the reduction of vanadium-extracted residues is shown in Table 1. Specifically, the Cr, V and C content are 3.8%, 3.6%, and 4.0%, respectively, along with trace amounts of Si and Mn.

Table 1. Typical composition of vanadium-chromium-containing hot metal/wt.%.

Element	C	Si	Mn	Cr	V
Content	4.0	0.5	0.5	3.8	3.6

The oxygen partial pressure required to achieve the equilibrium for vanadium extraction while preserving chromium in the hot metal of this composition is calculated as follows. The reaction for oxygen dissolution in hot metal and its corresponding Gibbs free energy change is expressed as:

$$O_2 = 2[O] \quad \Delta G_6^{\ominus} = -234.3 - 0.00578T \ \text{(kJ/mol)} \tag{6}$$

By linearly combining Equations (1) and (2) with Equation (6), the following equilibrium reactions and their Gibbs free energy changes are obtained:

$$O_2(g) + \frac{4}{3}[V] = \frac{2}{3}V_2O_3(s) \quad \Delta G_7^{\ominus} = -775.87 + 0.21T \ \text{(kJ/mol)} \tag{7}$$

$$O_2(g) + \frac{4}{3}[Cr] = \frac{2}{3}Cr_2O_3(s) \quad \Delta G_8^{\ominus} = -697.33 + 0.20T \ \text{(kJ/mol)} \tag{8}$$

Considering only the interaction of C, V and Cr, the interaction coefficients of C-Cr, Cr-Cr, C-V and V-V are as shown in Table 2.

Table 2. Interaction coefficients of C-Cr, Cr-Cr, C-V and V-V.

e_{Cr}^{C}	e_{Cr}^{Cr}	e_{V}^{C}	e_{V}^{V}
−0.12	−0.0003	−0.16	0.015

Based on the isothermal Equations (7) and (8), the oxygen partial pressure in equilibrium with the mass fractions ω[V] and ω[Cr] in the hot metal can be obtained:

$$(\lg p_{O_2})_v = \frac{2}{3}\lg\alpha_{V_2O_3} + 0.21\omega[C] + 0.02\omega[V] - \frac{4}{3}\lg\omega[V] - \frac{40521.30}{T} + 10.75 \tag{9}$$

$$(\lg p_{O_2})_{Cr} = \frac{2}{3}\lg\alpha_{Cr_2O_3} + 0.16\omega[C] + 0.0004\omega[Cr] - \frac{4}{3}\lg\omega[Cr] - \frac{36419.33}{T} + 10.19 \tag{10}$$

In Equations (9) and (10), $\alpha_{V_2O_3}$ and $\alpha_{Cr_2O_3}$ represent the activities of V_2O_3 and Cr_2O_3 in the slag, respectively. $\lg p_{O_2}$ denotes the equilibrium oxygen partial pressure, while ω[C] , ω[V] , and ω[Cr] correspond to the mass fractions of [C], [V], and [Cr], respectively.

Assuming $\alpha_{V_2O_3} = 1$ and $\alpha_{Cr_2O_3} = 1$, the following equations are obtained when $\omega[C] = 4\%$:

$$(\lg p_{O_2})_v = 0.02\omega[V] - \frac{4}{3}\lg\omega[V] - \frac{40521.30}{T} + 11.59 \tag{11}$$

$$(\lg p_{O_2})_{Cr} = 0.0004\omega[Cr] - \frac{4}{3}\lg\omega[Cr] - \frac{36419.33}{T} + 10.83 \tag{12}$$

By taking $\lg p_{O_2}$ as the vertical axis and ω[Cr] and ω[V] as the horizontal axes, Equations (11) and (12) are plotted in Figure 3.

 doi:10.20944/preprints202510.1670.v1

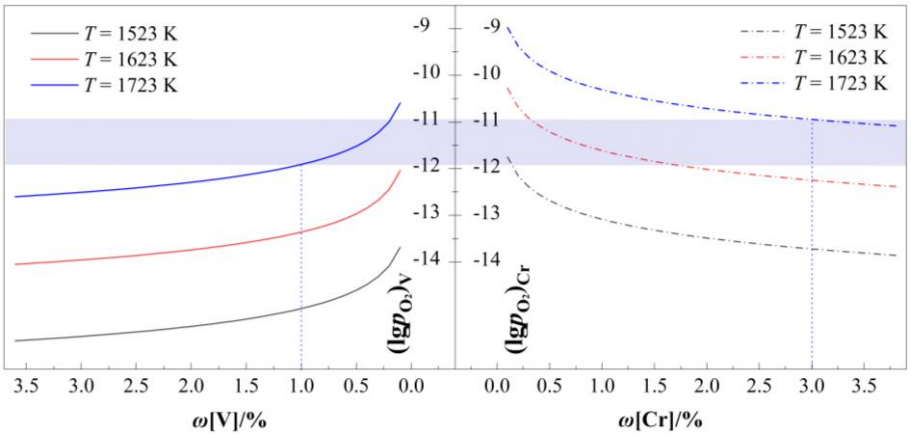

Figure 3. Oxygen partial pressure in equilibrium with [V] and [Cr] when ω[C] = 4%.

As demonstrated in Figure 3, the equilibrium oxygen partial pressures for vanadium oxidation($(\lg p_{O_2})_V$) and chromium oxidation ($(\lg p_{O_2})_{Cr}$) exhibit distinct dependencies on their respective solute concentrations (ω[V] and ω[Cr]) in the melt. Both $(\lg p_{O_2})_V$ and $(\lg p_{O_2})_{Cr}$ increase monotonically with decreasing ω[V] and ω[Cr], respectively. Notably, the rate of increase diverges significantly across concentration regimes: (1) At high solute concentrations (ω[V] > 1.0% and ω[Cr] > 1.0%), the oxygen partial pressures show gradual variations with composition; (2) Below the critical threshold of ω[V] < 1.0% or ω[Cr] < 1.0%, both $(\lg p_{O_2})_V$ and $(\lg p_{O_2})_{Cr}$ escalate rapidly, indicating enhanced thermodynamic driving forces for oxidation at dilute concentrations.

Importantly, a consistent hierarchy of oxygen partial pressure is observed across all temperatures: $(\lg p_{O_2})_V < (\lg p_{O_2})_{Cr}$. This thermodynamic hierarchy establishes an optimal oxygen partial pressure window ($(\lg p_{O_2})_V < \lg p_{O_2} < (\lg p_{O_2})_{Cr}$) for selective oxidation processes. Within this window, vanadium extraction can be prioritized while suppressing chromium loss, as exemplified by the 1723 K system: (1) The lower upper bound ($\lg p_{O_2} > -11.91$) ensures sufficient vanadium oxidation when ω[V] < 1.0%; (2) The upper bound ($\lg p_{O_2} < -10.94$) prevents chromium oxidation for ω[Cr] > 3.0%. Selecting 3.0% as the lower limit ensures that the oxygen partial pressure window remains sufficiently wide for experimental control; (3) The resultant operational window of $-11.91 < \lg p_{O_2} < -10.94$ demonstrates the feasibility of achieving concurrent vanadium extraction and chromium preservation through precise oxygen potential control.

In practical experiments, the oxygen partial pressure could be controlled by adjusting the CO-CO_2 gas ratio in the furnace atmosphere, or FeO content in slag.

3. Materials and Methods

3.1. Raw Materials

The initial melt was prepared using blast furnace (BF) powder, Ferrovanadium-50 (FeV50) and high carbon Ferrochrome (HC FeCr), all supplied by Shanxi Taisteel Stainless Steel co., LTD.. Table 3 summarizes the chemical compositions of these materials. The initial slag consisted of reagent-grade FeO, CaO, and SiO_2 powders (purity > 99%).

Table 3. Chemical composition of raw materials for initial melt preparation/wt.%.

Materials	Fe	V	Cr	C	Si	Mn	S	P
BF iron powder	88.50			4.00	0.5	0.5	0.005	0.005
FeV50 powder	47.10	50.00		0.65	1.45	0.48	0.03	0.04
HC FeCr powder	42.50		49.53	7.45				

 doi:10.20944/preprints202510.1670.v1

3.2. Experimental Apparatus

Experiments were conducted in a molybdenum-lined muffle resistance furnace (Model BFS-16, Beijing Fiame Temperature Technology Co., Ltd.) equipped with $MoSi_2$ heating elements. The furnace operates up to 1873 K with a temperature control accuracy of ±5 K (Figure 4).

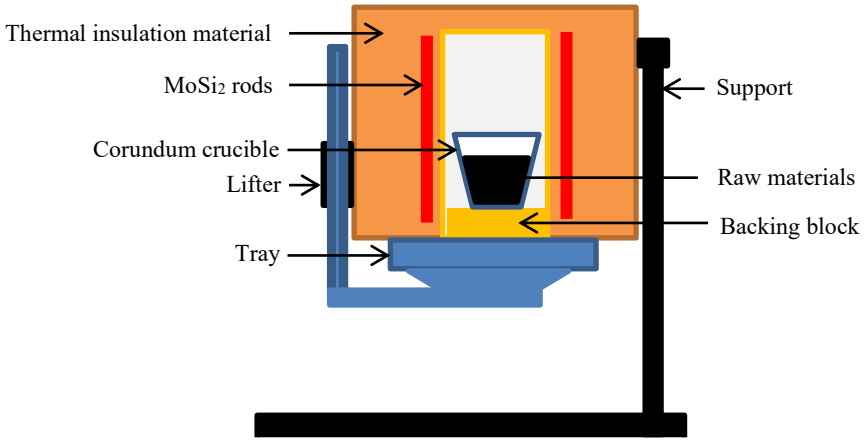

Figure 4. Schematic diagram of molybdenum muffle resistance furnace.

3.3. Experimental Design

As discussed in Section 2.1, the optimal temperature range for vanadium extraction while preserving chromium under standard conditions is 1517–1704 K. However, the temperatures corresponding to points A and B in Figure 1 are typically higher than those under standard conditions due to the influence of the hot metal composition. In order to ensure effective slag-metal separation during the experiments, the temperature range was set with a lower limit of 1633 K, an upper limit of 1753 K, and an interval of 30 K.

In this paper, FeO was selected as the oxidizing agent. The required amount of FeO consists of two components: one for oxidizing Si, Mn, and V, and the other is additional component for maintaining the oxygen potential equilibrium necessary to balance residual V and Cr. Based on calculations, for 100 g of hot metal, the theoretical FeO consumption for oxidizing Si, Mn, and V is 10.9 g. The FeO required to maintain the equilibrium for residual V and Cr is determined through the following calculations.

The relationship between the solubility of oxygen in hot metal and temperature is expressed as:

$$\lg\omega[\mathrm{O}] = -\frac{6320}{T} + 2.734 + \lg\alpha(\mathrm{FeO})\ [22] \tag{13}$$

where α(FeO) is the activitie of FeO in the slag. ω[O] can be derived from the equilibrium constant for the dissolution of O_2 in hot metal as shown in Equation (6). The equilibrium constant K_6 is expressed as:

$$K_4 = \frac{(p_{O_2})^{\frac{1}{2}}}{\alpha[\mathrm{O}]} \tag{14}$$

Since the dissolved oxygen in hot metal can be considered a dilute solution of [O], α[O] = ω[O]. Substituting Equations (6) and (14) into Equation (13) yields:

$$\lg\omega[\mathrm{O}] = \frac{1}{2}\lg p_{O_2} + \frac{117150 + 2.89T}{2.303\mathrm{R}T} \tag{15}$$

Substituting Equation (15) into Equation (13):

$$\lg\alpha(\mathrm{FeO}) = \frac{1}{2}\lg p_{O_2} + \frac{117150 + 2.89T}{2.303\mathrm{R}T} + \frac{6320}{T} - 2.73 \tag{16}$$

 doi:10.20944/preprints202510.1670.v1

At a temperature of 1723 K and an oxygen partial pressure $\lg p_{O_2}$ ranging from −11.91 atm to −10.94 atm (calculated in Section 2.2), α(FeO) is determined to between 0.048 and 0.147 according to Equation (16). For simplicity, the final slag was assumed to behave as an ideal solution, where α(FeO) is equal to its mole fraction. The final slag consists of CaO, SiO_2, FeO, V_2O_3, and MnO with their molar quantities denoted as n(CaO), $n(SiO_2)$, n(FeO), $n(V_2O_3)$, and n(MnO) respectively. Thus, α(FeO) can be expressed as:

$$\alpha(\mathrm{FeO}) = \frac{n(\mathrm{FeO})}{n(\mathrm{CaO}) + n(\mathrm{SiO_2}) + n(\mathrm{FeO}) + n(\mathrm{V_2O_3}) + n(\mathrm{MnO})} \quad (17)$$

Considering 100 g sample of vanadium-chromium-containing hot metal and 40 g of initial slag with a fixed basicity of (R_2: $\omega(\mathrm{CaO})/\omega(\mathrm{SiO_2})$) 1.8, n(FeO) is calculated via Equation (17) to span from 0.026 mol and 0.086 mol, corresponding to an FeO mass of approximately 2.23 g to 8.95 g, corresponding to ω(FeO) in final slag is 5.6−17.0%. Incorporating the FeO consumed during oxidation reactions, the total FeO requirement is estimated to be between 13.13 g and 19.85 g.

In this paper, a two-stage single-factor experimental design was adopted to systematically analyze the effects of temperature and FeO content on vanadium-chromium separation: (1) Temperature gradient experiment (Heat No. 1–5): Fitting ω(FeO) in final slag is 10.0%. Systematically varied temperature from 1633 K to 1753 K in 30 K intervals. This design isolates temperature as the sole variable to determine the thermal window for optimal vanadium oxidation and chromium retention; (2) FeO content gradient experiment (Heat No. 6–9): Fixed temperature at the optimal value identified in stage 1 (1723 K) and systematically varied ω(FeO) in final slag is 3.0-20.0%。 This stage focuses on optimizing FeO dosage to achieve the desired oxygen potential for selective oxidation. Each group of experiments was conducted three times.

The experimental plan was designed as shown in Table 4. CaO and SiO_2 were added to improve fluidity of the resultant slag. To reduce interactions with the corundum crucible, the slag's basicity was set at 1.8. This promotes a protective layer of $2CaO{\cdot}SiO_2$ at the interface, minimizing Al_2O_3 dissolution [23,24]. The hot metal mass was fixed at 100 g, with its composition detailed in Table 1.

Table 4. Experimental scheme.

Heat no.	Design Stage	Temperature/ K	ω(FeO) in final slag (set value), %	Initial slag, g			
				FeO	CaO	SiO_2	R_2
1	1 (Temp)	1633	10.0	14.9	19.8	9. 9	
2	1 (Temp)	1663	10.0	14.9	19.8	9. 9	
3	1 (Temp)	1693	10.0	14.9	19.8	9. 9	
4	1 (Temp)	1723	10.0	14.9	19.8	9. 9	
5	1 (Temp)	1753	10.0	14.9	19.8	9. 9	1.8
6	2 (FeO)	1723	3.0	12.1	21.6	10.9	
7	2 (FeO)	1723	5.0	12.9	21.0	10.6	
8	2 (FeO)	1723	15.0	17.1	18.3	9.1	
9	2 (FeO)	1723	20.0	19.1	17.1	8.4	

3.4. Experimental Procedure

All raw materials were thoroughly mixed and loaded into a corundum crucible. Once the furnace reached the predetermined experimental temperature, the crucible containing the sample was placed into the furnace, and the timing was started. After holding at the target temperature for 1 hour, the crucible was removed and cooled to room temperature. Then the crucible walls were visually inspected after the experiment and showed no significant signs of corrosion or slag penetration. The crucible was then carefully broken using a chisel. A clear interface between the metal phase (bottom) and slag phase (top) was observed in all samples, confirming effective phase separation. Representative samples were collected separately from the metal and slag phases for subsequent chemical and microstructural analysis.

 doi:10.20944/preprints202510.1670.v1

3.5. Calculation Methods

The oxidation rate η_M, representing the percentage of vanadium, chromium, and carbon oxidized, was calculated using the following formula:

$$\eta_M = \frac{\omega[M]^0 - \omega[M]}{\omega[M]^0} \times 100\% \quad (18)$$

where $\omega[M]^0$ is the initial mass fraction of the element in the hot metal (%), and $\omega[M]$ is the mass fraction in the hot metal after oxidation (%), with $\omega[V]$ set below 1%, that is, $\eta_V > 72.22\%$.

In order to achieve the goal of maximizing vanadium oxidation (η_V) while minimizing chromium oxidation (η_{Cr}) in hot metal, this paper introduces the vanadium-chromium separation index ($SI_{V\text{-}Cr}$) to quantify the degree of separation between vanadium and chromium. The calculation formula for $SI_{V\text{-}Cr}$ is provided in Equation (19):

$$SI_{V\text{-}Cr} = \sqrt{\eta_V \times (1 - \eta_{Cr})} \quad (19)$$

where η_V represents the extent of vanadium oxidation, and $(1-\eta_{Cr})$ reflects the degree of chromium retention. As a composite index, $SI_{V\text{-}Cr}$ evaluates the separation performance of vanadium and chromium through a geometric mean approach, emphasizing the simultaneous optimization of vanadium extraction and chromium retention. Specifically, a high $SI_{V\text{-}Cr}$ value indicates effective separation, characterized by high vanadium oxidation and low chromium oxidation. Conversely, a low $SI_{V\text{-}Cr}$ value suggests poor separation, with either low vanadium oxidation or high chromium oxidation.

The slag-metal distribution ratios of vanadium (L_V) and chromium (L_{Cr}) were calculated using the following equations:

$$L_V = \frac{\omega(V_2O_3)}{\omega[V]} \quad (20)$$

$$L_{Cr} = \frac{\omega(Cr_2O_3)}{\omega[Cr]} \quad (21)$$

where $\omega(V_2O_3)$ and $\omega(Cr_2O_3)$ are the mass fractions of V_2O_3 and Cr_2O_3 in the slag (%), respectively.

4. Results and Discussion

4.1. Effect of Temperature on Vanadium Extraction and Chromium Retention

4.1.1. Temperature-Dependent Oxidation and Separation of [V] and [Cr] in Hot Metal

The oxidation behavior of [V], [Cr], and [C] in hot metal was systematically investigated under a fixed ω(FeO) (10%) in final slag. The individual contents of carbon, vanadium, and chromium were fitted with temperature, as shown in Equations (22)–(24) and Figure 5a. While all three elements decrease in content as temperature rises, the behavior of vanadium diverges from that of chromium and carbon above 1693 K, where its rate of decline attenuates. This divergence may be attributed to carbon's relatively higher susceptibility to oxidation compared to vanadium at high temperatures. The determined operational window for achieving ω[V] ≤ 1%, as derived from Equation (23) and the experimental data, is 1693 K to 1753 K. Beyond this range, the vanadium content increases, confirming that these extreme temperatures inhibit effective vanadium oxidation.

$$\omega[Cr] = 3.49 \times 10^{-5}T^2 - 0.12T + 113.33 \quad (22)$$

$$\omega[V] = 7.45 \times 10^{-5}T^2 - 0.26T + 231.54 \quad (23)$$

$$\omega[C] = 3.97 \times 10^{-5}T^2 - 0.15T + 134.25 \quad (24)$$

 doi:10.20944/preprints202510.1670.v1

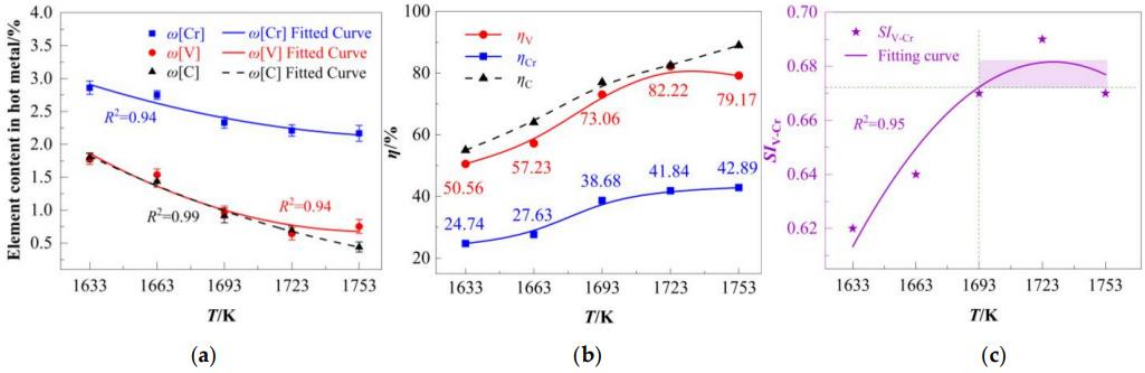

Figure 5. Effects of temperature on the oxidation separation of [V] and [Cr]: (**a**) Influence of temperature on ω[V], ω[Cr] and ω[C]; (**b**) Effect of temperature on η_V, η_{Cr} and η_C; (**c**) Impact of temperature on $SI_{V\text{-}Cr}$.

Figure 5b illustrates the temperature-dependent oxidation rates (η_V, η_{Cr} and η_C). η_C demonstrates the steepest positive correlation, rising linearly from 55% to 89% across the temperature range. η_V peaked at 82.2% at 1723 K (the optimal temperature for vanadium extraction), while η_{Cr} increases monotonically from 24.74% (1633 K) to 42.89% (1753 K), exhibiting near-linear progression above 1693 K. Across the entire temperature range, η_V consistently exceeded η_{Cr}, with a steeper increase in η_V (55.56% to 82.22%) compared to η_{Cr} (24.74% to 42.89%). This divergence stems from two factors: thermodynamic preference (Section 2.1) and the mediating role of carbon (detailed in Section 4.1.2).

Below 1723 K, η_V and η_C followed similar trends; however, above 1723 K, η_C surpassed η_V (Figure 5b). This inversion reflects intensified competition between [C] and [V] for oxygen at elevated temperatures [25,26].

The separation efficiency of [V] and [Cr], quantified by $SI_{V\text{-}Cr}$, as shown in Figure 5c. The fitting curve exhibits an upward convex characteristic and attains its peak at approximately 1723 K. The initial increase in $SI_{V\text{-}Cr}$ was driven by the rapid rise in η_V (50.56% to 82.22%), while η_{Cr} increased modestly (24.74% to 41.84%). Beyond 1723 K, $SI_{V\text{-}Cr}$ declined slightly primarily due to the reduction in η_V (82.22% to 79.17%) and marginal η_{Cr} increase (41.84% to 42.89%). According to the quadratic fitting relationship:

$$SI_{V\text{-}Cr} = -7.55 \times 10^{-5} T^2 + 0.03T - 21.87 \quad (25)$$

Within the temperature range of 1693 K ≤ T ≤ 1753 K, $SI_{V\text{-}Cr}$ can be maintained within the range of 0.67 to 0.69. These results underscore the adverse effects of excessive temperatures on vanadium oxidation selectivity, thereby reducing the separation efficiency.

The optimal process window was determined as 1693–1753 K, where $SI_{V\text{-}Cr}$ exceeded 0.67, η_V remained above 73.06%, and η_{Cr} was suppressed below 42.89%. At same time, ω[V] was reduced to <0.97%, while ω[Cr] remained >2.17%. These results indicate that effective separation of vanadium and chromium in hot metal has been achieved under the specified conditions.

It should be noted that the discussion on the influence of temperature in this section is based on the condition of a fixed ω(FeO) (10%). The boundaries of this optimal temperature window (1693–1753 K) are essentially the result of the competition between the thermodynamics of V and Cr oxidations in this specific oxygen potential. It can be predicted that when the initial oxygen potential (such as FeO content) changes, the oxidation behavior of carbon and the oxidation competition between V and Cr will also change accordingly, leading to a shift in the optimal temperature range. For example, at a higher FeO dosage, to avoid excessive oxidation of Cr, the upper limit of the optimal temperature may need to be appropriately reduced.

 doi:10.20944/preprints202510.1670.v1

4.1.2. Carbon-Mediated Vanadium Extraction and Chromium Retention

To systematically assess the role of carbon as a medium for vanadium extraction and chromium protection, we introduced two empirical indices: the vanadium extraction efficiency per unit carbon oxidation rate (η_V/η_C) and the protected chromium per unit residual carbon content ($(1-\eta_{Cr})/\omega[C]$), as illustrated in Figure 6. The value of $\omega[Cr]/\omega[C]$ exhibits a monotonic increase with rising temperature, climbing from 1.59 at 1633 K to 4.93 at 1753 K, which suggests an enhanced protective effect of carbon on chromium under higher temperatures. In contrast, η_V/η_C demonstrates less temperature sensitivity than $(1-\eta_{Cr})/\omega[C]$, following an initial increase followed by a decline. Beyond 1723 K, the efficacy of carbon in extracting vanadium diminishes. The net effect of carbon accounts for the markedly higher temperature sensitivity observed in the oxidation of vanadium compared to chromium.

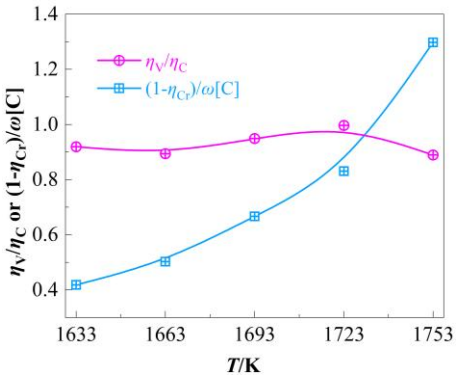

Figure 6. Effect of carbon on vanadium extraction and chromium retention.

4.1.3. Temperature-Dependent Migration Behavior of Vanadium and Chromium

The migration behavior of vanadium and chromium oxides in the slag phase was critically influenced by temperature variations, as summarized in Figure 7.

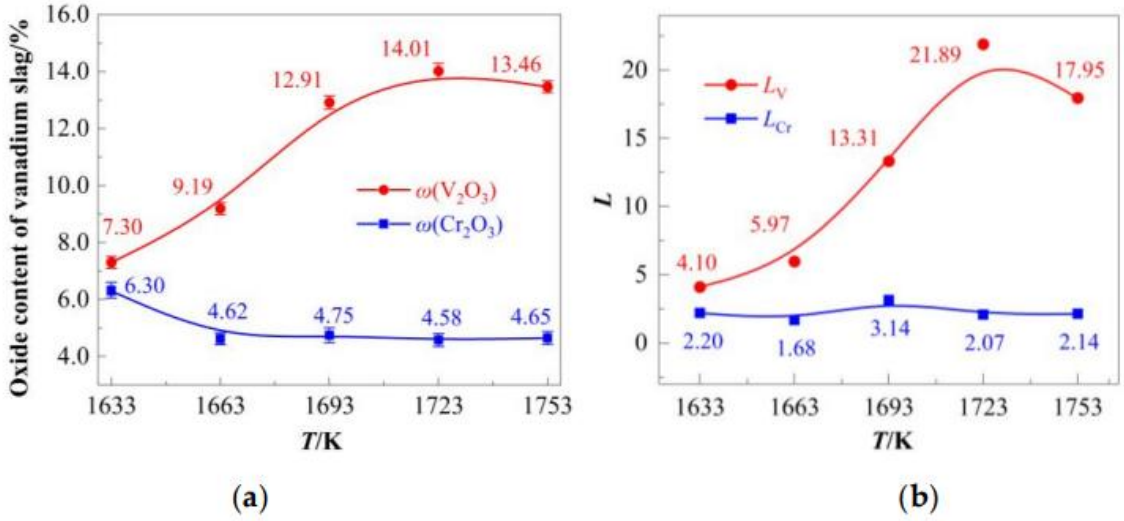

Figure 7. Effect of temperature on vanadium chromium migration: (**a**) Effect of temperature on the content of V_2O_3 and Cr_2O_3 in the final slag, (**b**) Effect of temperature on the slag-gold partition ratio.

The V_2O_3 content in the slag initially increased with rising temperature, peaking at 14.01% (1723 K), followed by a slight decline to 13.46% at 1753 K (Figure 7a). In contrast, Cr_2O_3 content exhibited a gradual reduction from 6.30% (1623 K) to 4.65% (1753 K). Correspondingly, L_V surged from 4.10 (1623

 doi:10.20944/preprints202510.1670.v1

K) to 21.89 (1723 K), then decreased to 17.95 (1753 K), while L_{Cr} remained relatively stable within a narrow range (1.68–3.14) across the tested temperatures (Figure 7b). These results demonstrate that moderate temperature elevation (<1723 K) significantly enhances vanadium partitioning into the slag, whereas chromium migration is minimally affected.

Within the optimized temperature window (1693–1753 K), V_2O_3 content stabilized between 12.91% and 14.01%, while Cr_2O_3 content varied from 4.58% to 4.75%. Notably, despite the temperature-dependent increase in chromium oxidation rate (Section 4.1.1), oxidized chromium exhibited incomplete migration to the slag phase.

4.2. Effect of FeO Content on Vanadium Extraction and Chromium Retention

4.2.1. FeO-Dependent Oxidative Separation of [V] and [Cr]

The oxidative separation of [V] and [Cr] in hot metal was systematically investigated under varying ω(FeO) at 1723 K, as summarized in Figure 8.

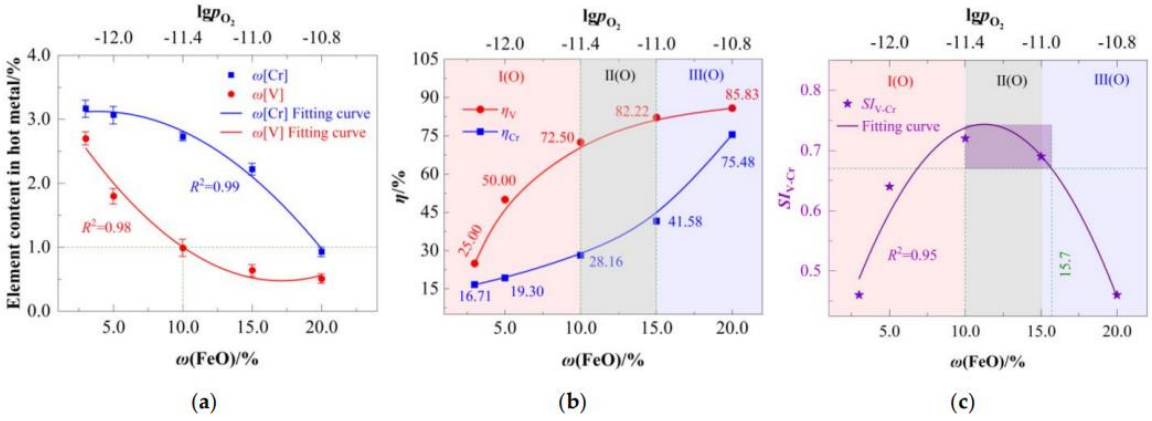

Figure 8. Influence of ω(FeO) on the oxidative separation of [V] and [Cr]: (**a**) Residual ω[V] and ω[Cr] in hot metal, (**b**) η_V and η_{Cr}, (**c**) $SI_{V\text{-}Cr}$ index.

Figure 8a illustrates the equilibrium between slag oxygen potential and residual element content of hot metal. Both ω[V] and ω[Cr] exhibit pronounced decreasing trends with increasing ω(FeO). Empirical relationship between ω[V] and ω(FeO) was established using Equation (26):

$$\omega[V] = 0.01\omega(FeO)^2 - 0.36\omega(FeO) + 3.52 \quad (26)$$

Based on Equation (26) and the experimental data, it is determined that ω[V] dropped below the critical threshold of 1.0% only when ω(FeO) exceeded 10%, the corresponding oxygen partial pressure $\lg p_{O_2}$ = –11.42. This value exceeds the theoretical prediction (–11.91) due to idealized assumptions in the model and competitive FeO consumption by carbon oxidation. Thus, efficient vanadium extraction requires higher oxygen potential than theoretically projected.

Figure 8b plots η_V and η_{Cr} against ω(FeO). Although both efficiencies increase with ω(FeO), their response curves differ significantly — η_V exhibits a convex upward trend, in contrast to the concave downward trend of η_{Cr}. These distinct behaviors form the basis for defining the three characteristic regions listed in Table 7.

Table 7. Characteristic regions defined by η_V and η_{Cr} oxidation behavior versus ω(FeO).

Region	Name	ω(FeO) Range	Dominant Process	η_V/η_{Cr}
Ⅰ(O)	V-Dominant Zone	3–10%	Vanadium Preferential Oxidation	2.5–3.1
Ⅱ(O)	Cr-Activation Zone	10–15%	Chromium Oxidation Activation	1.8–2.4
Ⅲ(O)	Cr-Runaway Zone	>15%	Chromium Massive Oxidation	<1.1

 doi:10.20944/preprints202510.1670.v1

- Region I(O) (V-Dominant Zone, ω(FeO) = 3–10%): η_V rises sharply due to preferential vanadium oxidation (thermodynamically favored; Section 2.2), while η_{Cr} increases marginally.
- Region II(O) (Cr-Activation Zone, ω(FeO) = 10–15%): η_{Cr} oxidation accelerates.
- Region III(O) (Cr-Runaway Zone, ω(FeO) > 15%): η_{Cr} undergoes rapid escalation, indicating exceedance of chromium's oxidation threshold.

This divergence underscores the core mechanism of selective oxidation: Vanadium oxidizes readily at low oxygen potentials, whereas chromium requires significantly higher potentials for massive oxidation. Precise oxygen potential control thus enables targeted vanadium extraction with chromium retention.

Figure 8c reveals a non-monotonic trend in $SI_{V\text{-}Cr}$, which peaks then declines with increasing ω(FeO). The relationship is fitted by:

$$SI_{V\text{-}Cr} = -0.004\ \omega(FeO)^2 + 0.084\omega(FeO) + 0.268 \quad (25)$$

Maximizing $dSI_{V\text{-}Cr}/d\omega(FeO) = 0$ yields a distinct selectivity peak ($SI_{V\text{-}Cr} = 0.74$) at ω(FeO) = 10.5%. Suboptimal oxidation occurs at ω(FeO) < 10.5%, while ω(FeO) > 15.7% promotes excessive Cr oxidation, degrading selectivity.

Thus, effective V/Cr separation ($SI_{V\text{-}Cr} \geq 0.67$) requires an operational window of ω(FeO) = 10.0–15.7%, corresponding to $\lg p_{O_2}$ = –11.4 to –10.9. This range spans "Region II(O)" and early "Region III(O)". Although chromium begins to oxidize at an FeO concentration of 15%, the practically feasible range is extended to 15.7%. This indicates that FeO can vary by ±0.35% without compromising process stability. Such a tolerance not only enhances the operational flexibility but also guarantees the efficient extraction of vanadium, highlighting its critical role in process control.

Within this window: (1) η_V > 72.22%, η_{Cr} < 41.58%; (2) ω[V] < 1.0%, ω[Cr] > 2.3%, The requisite oxygen supply (33.1–38.2 kg/tFe) is 27.7–81.1% lower than conventional converter-based vanadium extraction (43.0–195.0 kg/tFe, accounting for 70–90% utilization efficiency [27]). This demonstrates the feasibility of low-oxygen-potential vanadium extraction with minimal chromium loss—a significant advance toward sustainable refining of high-chromium hot metal.

The optimal operating window of FeO (10–15.7%) determined in this study was obtained at a fixed temperature of 1723 K. Temperature plays a crucial role as it directly affects the equilibrium constant and kinetic rate of the reaction. At higher temperatures, the reducing power of carbon increases, which may enable the same V oxidation efficiency with a lower FeO dosage while better suppressing the oxidation of Cr. Conversely, at lower temperatures, a higher FeO content may be required to compensate for the insufficient reaction kinetics, but this significantly increases the risk of Cr oxidation. Therefore, the control range of FeO is not constant but is closely coupled with temperature.

4.2.2. FeO-Dependent Migration of Vanadium and Chromium

The migration behavior of vanadium and chromium oxides into the slag phase under varying ω(FeO) is illustrated in Figure 9. As ω(FeO) increased, both V_2O_3 and Cr_2O_3 contents in the slag rose (Figure 9a), driven by enhanced oxidative capacity of the slag. L_V surged from 1.22 (3.0% FeO) to 22.28 (15% FeO), with no obvious bending point (Figure 8b). While chromium migration L_{Cr} exhibited a milder increase (1.68–4.58), with a distinct inflection at 15% ω(FeO) (Figure 9b). This indicates that FeO promotes vanadium migration to slag, but low dose ω(FeO) (15%) has no significant effect on chromium migration.

 doi:10.20944/preprints202510.1670.v1

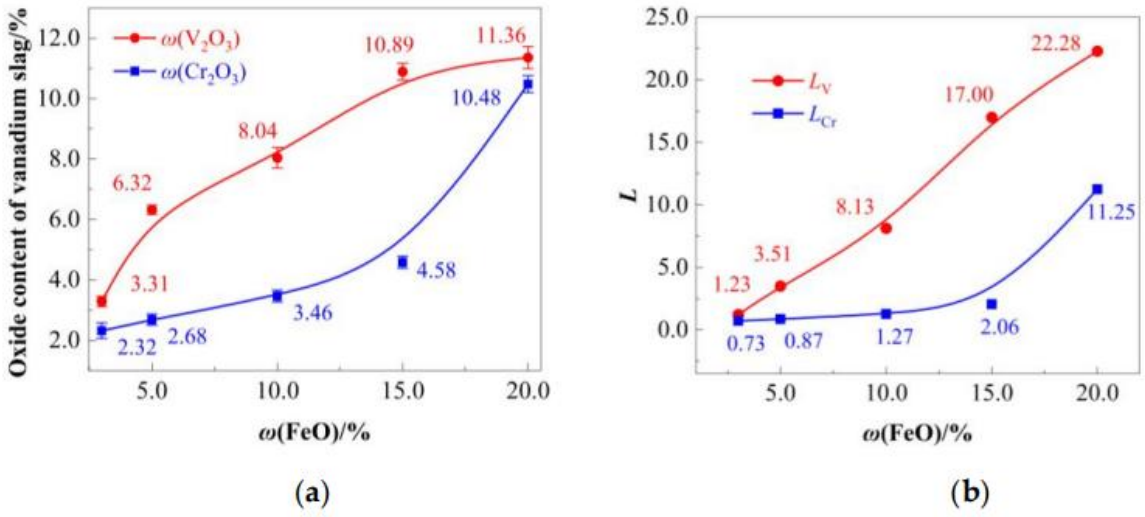

Figure 9. Influence of ω(FeO) dosage on vanadium and chromium migration: (**a**) V_2O_3 and Cr_2O_3 content in final slag, (**b**) Distribution ratios (L_V and L_{Cr}).

Within the optimized ω(FeO) range of 10–15.7% identified in Section 4.2.1, the vanadium-chromium slag achieves $\omega(V_2O_3)$ values of 8.04–10.88% and $\omega(Cr_2O_3)$ values of 3.46–4.58%.

4.3. Comprehensive Discussion on the Synergistic Control of Temperature and Oxygen Potential

The experimental design of this study adopted the single-factor variable method, which separately revealed the independent influence laws of temperature and FeO dosage on the separation of V-Cr. However, the success of industrial applications relies on the coordinated control of these two key parameters.

A more scientific process control strategy should be regarded as a dynamic optimization process: higher operating temperatures create favorable thermodynamic and kinetic conditions for achieving "low oxygen potential extraction of V", allowing for the use of lower FeO dosages, thereby achieving efficient extraction of V while maximizing the utilization of carbon's protective effect on Cr; while operating at lower temperatures, the system is forced into the "high oxygen potential extraction of V" mode, at which the risk of Cr loss significantly increases.

Therefore, the temperature window (1693–1753 K) and FeO window (10–15.7%) determined in this study should be understood as a guiding parameter space. Its core value lies in revealing that the combination of "high temperature - medium-low FeO" is a more optimal path for selective oxidation. Future research can further precisely quantify this coupling relationship through experimental designs such as response surface methodology (RSM) and construct a more accurate mathematical model to guide industrial production.

4.4. Comparative Analysis of Vanadium Extraction and Chromium Retention (VECR) Process with Conventional Methods

A systematic comparison between the proposed VECR process and traditional vanadium extraction methods is summarized in Table 8. The primary differences between these two processes lie in the control of temperature and oxygen potential, and the difference of oxidation rate and composition of vanadium chromium slag caused by these factors.

Table 8. Comparison of process parameters and results of VECR process with traditional process.

Parameter	Traditional Process	VECR Process	Improvement
Temperature/K	1623–1693 [27,28]	1693–1753	+65 K (optimized oxidation)
Oxygen supply/kg·(tFe)$^{-1}$	43.0–195.0	33.1–38.2	>80 kg/tFe reduction

 doi:10.20944/preprints202510.1670.v1

Parameter	Traditional Process	VECR Process	Improvement
η_V/%	75.0–90.0 [27]	72.5–82.2	Comparable efficiency
η_{Cr}/%	50.0–70.0 [29]	28.2–42.9	>40% reduction
$\omega(V_2O_3)$/%	8.2–16.5 [30,31]	10.9–14.0	Higher purity
$\omega(Cr_2O_3)$/%	5.0–10.0	3.5–7.3	Meets low-Cr standards

The VECR process is about 65 K higher than the traditional process. In traditional processes, the temperature is typically maintained below the C-V oxidation transition temperature. In contrast, the VECR process requires the temperature to be controlled nearly C-V oxidation temperature, to ensure maximum $SI_{V\text{-}Cr}$.

Traditional processes involve a relatively high oxygen supply (43.0–195.0 kg/tFe) (as described section in 4.2.1) to create a high-oxygen-potential environment, which promotes vanadium oxidation. However, such conditions also significantly increase the chromium oxidation rate (50–70%), leading to a higher chromium content in the vanadium-slag (5–14%). This not only reduces the recovery value of the vanadium slag but also complicates subsequent chromium recovery. Furthermore, the high oxygen potential and elevated temperatures accelerate equipment wear and increase maintenance costs. In comparison, the VECR process reduces the oxygen supply to 33.1–38.2 kg/tFe, achieving effective vanadium oxidation (η_V: 72.5–82.2%) under low-oxygen-potential conditions while significantly lowering η_{Cr} (< 42.9%).

The VECR process significantly reduces oxygen consumption and chromium oxidation losses. Compared to conventional processes, the oxygen consumption of the VECR process is reduced by more than 80 kg/tFe, η_{Cr} is reduced by over 40%. This results in improved purity of the vanadium slag. In the vanadium slag formed by VECR process, $\omega(V_2O_3)$ is 10.88–14.01%, $\omega(Cr_2O_3)$ is 3.5–7.3%. These values satisfy the requirements for the recycling and utilization of low-chromium vanadium-chromium slag. Specifically, vanadium slag is considered to have industrial extraction value only when the V_2O_5 content exceeds 10% [32,33] (equivalent to V_2O_3 content 8.2%). Additionally, the Cr_2O_3 content in low-chromium vanadium-chromium slag is typically required to be less than 8% [34].

However, the VECR process also has certain limitations. For instance, under low-oxygen-potential conditions, the reaction rate is relatively slow, potentially requiring a longer reaction time and thereby impacting production efficiency.

Overall, the VECR process demonstrates significant advantages in terms of chromium retention and cost-effective production. By reducing the chromium oxidation rate, this process not only minimizes chromium resource waste, but also achieves efficient resource utilization. Moreover, the lower oxygen supply significantly reduces energy consumption and carbon emissions, aligning with the principles of green metallurgy. From an industrial application perspective, the VECR process is particularly suitable for production scenarios with high demands for vanadium and chromium resource utilization efficiency, especially in regions where chromium resources are scarce or environmental regulations are stringent. In the future, the promotion of this process is expected to achieve broader applications in the steel and metallurgical industries and provide valuable insights for the development of green metallurgical technologies.

5. Conclusions

This study successfully developed and validated a novel pyrometallurgical strategy for the synchronous extraction of vanadium and retention of chromium from high V-Cr hot metal through precise control of selective oxidation. The combined thermodynamic and experimental investigation led to the following key findings:

The thermodynamic analysis established that the temperature window of 1517–1704 K is critical, as it enables boron to function as an effective redox mediator. Within this regime, the oxidation priority of [V] > [C] > [Cr] creates a thermodynamic pathway for selective V extraction. Furthermore, there is a hierarchy of oxygen partial pressure required for the oxidation of vanadium and chromium. An optimal oxygen partial pressure window of -11.91 to -10.94 (logarithmic scale) at 1723 K was

 doi:10.20944/preprints202510.1670.v1

identified to achieve high V oxidation while suppressing Cr loss. This theoretical prediction provides a key parameter window for the optimization of experimental conditions, and its core conclusion is directly verified in subsequent experiments.

Temperature-dependent experiments demonstrate differential responses of η_V and η_{Cr}: vanadium oxidation exhibits higher temperature sensitivity than chromium, a phenomenon attributed to the stronger protective effect of carbon on chromium, rather than its promoting effect on vanadium extraction. The optimal temperature range is 1693–1753 K ($SI_{V\text{-}Cr} > 0.67$). In the low-temperature region (<1693 K), vanadium oxidation is incomplete, whereas in the high-temperature region (> 1753 K), the separation efficiency deteriorates.

Both η_V and η_{Cr} increase with the addition of FeO, with η_V consistently exceeding η_{Cr}. [V] oxidation occurring preferentially at lower FeO dosages. The optimal FeO dosage range is determined to be 10.0–15.7%. FeO contents exceeding this range lead to over-oxidation of [Cr], while insufficient FeO additions result in incomplete [V] oxidation.

Under optimized process conditions, η_V exceeds 72.5%, while η_{Cr} remains below 42.9%. These conditions result in a reduction of ω[V] to be less than 1%, while ω[Cr] remains above 2.17%. Additionally, $\omega(V_2O_3)$ and $\omega(Cr_2O_3)$ are 10.88–14.01%, and 3.46–7.31%, respectively, meeting the criteria for recycling low-chromium vanadium slag. These results demonstrate the effectiveness of the process in selectively oxidizing vanadium while minimizing chromium oxidation losses.

Compared to traditional processes, the proposed VECR method demonstrates significant advantages. It reduces oxygen consumption by over 80 kg/tFe and cuts Cr oxidation losses by more than 40%, directly translating to lower operational costs and enhanced resource utilization. The resulting V-Cr slag, with 10.88–14.01% V_2O_3 and 3.5–7.3% Cr_2O_3, meets the industrial standard for low-Cr feedstock. Most importantly, this process completely eliminates the need for the energy-intensive roasting and complex hydrometallurgical steps, offering a shorter, cleaner, and more economical flowsheet.

Author Contributions: Conceptualization, H.Z., D.Y. and Y.Q.; methodology, H.Z.; investigation, H.Z., Q.L. and F.W.; data curation, H.Z., X.W., L.W. and Q.L.; writing—original draft preparation, X.W. and H.Z.; writing—review and editing, X.W., L.W. and Y.Q.; visualization, L.W. and H.Z.; supervision, Y.Q. and F.W.; project administration, Y.Q.; funding acquisition, D.Y. and Y.Q. All authors have read and agreed to the published version of the manuscript.

Funding: This research was funded National Key Research and Development Program of China (2017YFB0603805)

Data Availability Statement: The raw data supporting the conclusions of this article will be made available by the authors on request.

Conflicts of Interest: The authors declare no conflict of interest.

References

1. Wang, G.; Diao, J.; Liu, L.; Li, M.; Li, H.; Li, G.; Xie, B. Highly efficient utilization of hazardous vanadium extraction tailings containing high chromium concentrations by carbothermic reduction. *Journal of Cleaner Production* **2019**, *237*, 117832.
2. Xiang, J.; Huang, Q.; Lv, W.; Pei, G.; Lv, X.; Bai, C. Recovery of tailings from the vanadium extraction process by carbothermic reduction method: Thermodynamic, experimental and hazardous potential assessment. *Journal of Hazardous Materials* **2018**, *357*, 128–137.
3. Xiang, J.; Huang, Q.; Lv, W.; Pei, G.; Lv, X.; Liu, S. Co-recovery of iron, chromium, and vanadium from vanadium tailings by semi-molten reduction–magnetic separation process. *Canadian Metallurgical Quarterly* **2018**, *57*, 262–273.
4. Zhang, B.; Wang, R.; Liu, C.; Jiang, M. Self-digestion of Cr-bearing vanadium slag processing residue via hot metal pre-treatment in steelmaking process. *Metallurgical and Materials Transactions B* **2022**, *53*, 1183–1195.

 doi:10.20944/preprints202510.1670.v1

5. Jing, J.; Guo, Y.; Wang, S.; Li, G.; Chen, F.; Yang, L.; Wang, C. Chromium and iron recovery from hazardous extracted vanadium tailings via direct reduction magnetic separation. *Journal of Environmental Chemical Engineering* **2023**, *11*, 110047.
6. A, X.W.W.; B, M.E.Y.A.; A, Y.Q.M.; A, D.X.G.; A, M.Y.W.; C, Z.B.F. Cyclic metallurgical process for extracting V and Cr from vanadium slag: Part I. Separation and recovery of V from chromium-containing vanadate solution. *Transactions of Nonferrous Metals Society of China* **2021**, *31*, 807–816.
7. Liu, L.; Kauppinen, T.; Tynjälä, P.; Hu, T.; Lassi, U. Water leaching of roasted vanadium slag: Desiliconization and precipitation of ammonium vanadate from vanadium solution. *Hydrometallurgy* **2023**, *215*, 105989.
8. An, Y.; Ma, B.; Zhou, Z.; Chen, Y.; Wang, C.; Wang, B.; Gao, M.; Feng, G. Extraction of vanadium from vanadium slag by sodium roasting-ammonium sulfate leaching and removal of impurities from weakly alkaline leach solution. *Journal of Environmental Chemical Engineering* **2023**, *11*, 110458.
9. Wang, Z.; Li, Z.; Chen, L.; Zhu, Y.; Wu, K.; Luo, D. Optimization and kinetic analysis of co-extraction of vanadium (IV) and chromium (III) from high chromium vanadium slag with titanium dioxide waste acid. *Minerals Engineering* **2025**, *233*, 109604.
10. Zhao, W.; Zhao, Z.; Xu, Y.; Cao, Z.; Li, W.; Zhao, T. A sustainable chromium and vanadium extraction and separation process from high-chromium vanadium slag via synchronous roasting and asynchronous leaching. *Separation and Purification Technology* **2025**, *368*, 133020.
11. Li, C.; Jiang, T.; Wen, J.; Yu, T.; Li, F. Review of leaching, separation and recovery of vanadium from roasted products of vanadium slag. *Hydrometallurgy* **2024**, 106313.
12. Zhang, X.; Meng, F.; Zhu, Z.; Chen, D.; Zhao, H.; Liu, Y.; Zhen, Y.; Qi, T.; Zheng, S.; Wang, M. A novel process to prepare high-purity vanadyl sulfate electrolyte from leach liquor of sodium-roasted vanadium slag. *Hydrometallurgy* **2022**, *208*, 105805.
13. Cheng, J.; Li, H.-Y.; Chen, X.-M.; Hai, D.; Diao, J.; Xie, B. Eco-friendly chromium recovery from hazardous chromium-containing vanadium extraction tailings via low-dosage roasting. *Process Safety and Environmental Protection* **2022**, *164*, 818–826.
14. Jiang, L.; Du, G.-C.; Wang, J.-P.; Wu, Z.-X.; Li, H.-Y. Eco-friendly efficient separation of Cr (VI) from industrial sodium vanadate leaching liquor for resource valorization. *Separation and Purification Technology* **2025**, *361*, 131673.
15. Hui, X.; Zhang, J.; Liang, Y.; Chang, Y.; Zhang, W.; Zhang, G. Comparison and evaluation of vanadium extraction from the calcification roasted vanadium slag with carbonation leaching and sulfuric acid leaching. *Separation and Purification Technology* **2022**, *297*, 121466.
16. Li, H.; Ren, Q.; Tian, J.; Tian, S.; Wang, J.; Zhu, X.; Shang, Y.; Liu, J.; Fu, L. Efficient recovery of vanadium from calcification roasted-acid leaching tailings enhanced by ultrasound in H2SO4-H2O2 system. *Minerals Engineering* **2024**, *205*, 108492.
17. Liu, S.; Wang, L.; Chen, J.; Ye, L.; Du, J. Research progress of vanadium extraction processes from vanadium slag: A review. *Separation and Purification Technology* **2024**, *342*, 127035.
18. Wang, C.; Guo, Y.; Wang, S.; Chen, F.; Yang, L.; Zheng, Y. Removal of sodium from vanadium tailings by calcification roasting in reducing atmosphere. *Materials* **2023**, *16*, 986.
19. Yao, Z.; Zhang, Q.; Wang, L.; Zhang, W.; Ma, B.; Wang, C. Non-salt roasting mechanism of V–Cr slag toward efficient selective extraction of vanadium. *Journal of Industrial and Engineering Chemistry* **2023**, *126*, 588–600.
20. Wan, J.; Du, H.; Gao, F.; Wang, S.; Zhang, Y. Direct Leaching of Vanadium from Vanadium-bearing Steel Slag Using NaOH Solutions: A Case Study. *Mineral Processing and Extractive Metallurgy Review* **2020**, 1–11.
21. Kunikata, Y.; Morita, K.; Tsukihashi, F.; Sano, N. Equilibrium Distribution Ratios of Phosphorus and Chromium between BaO-MnO Melts and Carbon Saturated Fe-Cr-Mn Alloys at 1 573 K. *ISIJ International* **2007**, *34*, 810–814.
22. Jost, W. *Physical Chemistry An Advanced Treatise*; Elsevier: 2012.
23. Chimenos, J.M.; Cuspoca, F.; Maldonado-Alameda, A.; Mañosa, J.; Rosell, J.R.; Andrés, A.; Faneca, G.; Cabeza, L.F. MSW incineration bottom ash-based alkali-activated binders as an eco-efficient alternative for urban furniture and paving: closing the loop towards sustainable construction solutions. *Buildings* **2025**, *15*, 1571.

 doi:10.20944/preprints202510.1670.v1

24. Ibrahim, I.K.; Rady, M.; Tawfik, N.M.; Kassem, M.; Mahfouz, S.Y. Enhancing strength and sustainability of concrete with steel slag aggregate. *Scientific Reports* **2025**, *15*, 17068.
25. Monfort, O.; Petrisková, P. Binary and ternary vanadium oxides: general overview, physical properties, and photochemical processes for environmental applications. *Processes* **2021**, *9*, 214.
26. Zhou, Z.-Y.; Tang, P. Optimization on temperature strategy of BOF vanadium extraction to enhance vanadium yield with minimum carbon loss. *Metals* **2021**, *11*, 906.
27. Zhou, Z.-y.; Tang, P.; Hou, Z.-b.; Wen, G.-h. Investigation of the end-point temperature control based on the critical temperature of vanadium oxidation during the vanadium extraction process in BOF. *Transactions of the Indian Institute of Metals* **2018**, *71*, 1957–1961.
28. Zhao, J.; Wu, W.; Zhao, B.; Li, X.; Xiao, F. Influence of Vanadium Extraction Converter Process Optimization on Vanadium Extraction Effect. *Metals* **2022**, *12*, 2061.
29. Farah, H.; Brungs, M. Oxidation-reduction equilibria of vanadium in CaO-SiO 2, CaO-Al 2 O 3-SiO 2 and CaO-MgO-SiO 2 melts. *Journal of materials science* **2003**, *38*, 1885–1894.
30. Wang, G.; Lin, M.-M.; Diao, J.; Li, H.-Y.; Xie, B.; Li, G. Novel strategy for green comprehensive utilization of vanadium slag with high-content chromium. *ACS Sustainable Chemistry & Engineering* **2019**, *7*, 18133–18141.
31. Wen, J.; Sun, Y.; Ning, P.; Xu, G.; Sun, S.; Sun, Z.; Cao, H. Deep understanding of sustainable vanadium recovery from chrome vanadium slag: Promotive action of competitive chromium species for vanadium solvent extraction. *Journal of Hazardous Materials* **2022**, *422*, 126791.
32. Lee, J.-c.; Kim, E.-y.; Chung, K.W.; Kim, R.; Jeon, H.-S. A review on the metallurgical recycling of vanadium from slags: towards a sustainable vanadium production. *Journal of Materials Research and Technology* **2021**, *12*, 343–364.
33. Namasivayam, C.; Prathap, K. Recycling Fe (III)/Cr (III) hydroxide, an industrial solid waste for the removal of phosphate from water. *Journal of hazardous materials* **2005**, *123*, 127–134.
34. Liu, W.; Wang, Z.; Cao, W.; Liang, Y.; Rohani, S.; Xin, Y.; Hua, J.; Ding, C.; Lv, X. Green and efficient separation of vanadium and chromium from high-chromium vanadium slag: a review of recent developments. *Green Chemistry* **2024**, *26*, 10006–10028.